# Ion fragmentation study of [EMMIM][TFSI], [EMIM][OTf] and [EMIM][DCA] by vacuum ultraviolet light

M. Kook[1], I. Kuusik[1], R. Pärna[1], T. Käämbre[1], A. Kikas[1], A. Tõnisoo[1], J. M. Kahk[1], A. Kivimäki[2,3], L. Reisberg[1] and V. Kisand[1]

[1]Institute of Physics, University of Tartu, W. Ostwald 1, EE-50411 Tartu, Estonia
[2]Nano and Molecular Systems Research Unit, University of Oulu, P.O. Box 3000, 90014 Oulu, Finland
[3]MAX IV Laboratory, Lund University, P.O. Box 118, 22100 Lund, Sweden

**Abstract**
The ionic liquids (ILs) 1-Ethyl-2,3-dimethylimidazolium bis(trifluoromethylsulfonyl)imide [EMMIM][TFSI], 1-Ethyl-3-methylimidazolium trifluoromethanesulfonate [EMIM][OTf] and 1-Ethyl-3-methylimidazolium dicyanamide [EMIM][DCA] were evaporated by effusion and a time-of-flight (TOF) instrument was employed as the mass analyzer while vacuum ultraviolet (VUV) light in the energy range 9 - 20 eV was used to excite the IL molecules. Fragmentation patterns with respect to excitation energy are discussed and decomposition products are analyzed. Hydrogenated and dehydrogenated fragments are discussed. Our experiment seems to show that the ionic liquids with larger anions have less cation fragmentation. [EMMIM][TFSI] was studied for the first time and it produces different fragments than 1-Ethyl-3-methylimidazolium based ionic liquids. Surprisingly 1-Ethyl-3-methylimidazolium or 1-Ethyl-2-methylimidazolium cations were not detected in the [EMMIM][TFSI] fragmentation pattern.

**Keywords:** time-of-flight mass spectrometry, ionic liquids, [EMMIM][TFSI], [EMIM][OTf], [EMIM][DCA]

## 1. Introduction

Ionic liquids (ILs) are generally defined as molten organic salts with a melting point below 100 °C. These compounds have attracted significant interest in the last few decades because of their uncommon physicochemical properties such as low melting temperatures, excellent solvation ability, relatively high thermal stability, low vapor pressure, non-flammability, and high electrochemical stability [1].

ILs have several applications in diverse fields, such as electrochemistry, nanotribology, synthesis, catalysis, green chemistry, nanotechnology, solar cells, fuel cells, batteries and ionic propulsion. With the availability of many suitable anions and cations, it is possible to synthesize a vast number of different ILs with designed properties. A promising application of ionic liquids is in lubricants. As ILs are highly polar, they can form a very strong effective adsorption film on specific metal surfaces, which contributes to their prominent anti-wear capability [2]. Because of their low volatility ILs are applicable under vacuum and are especially useful in spacecraft applications [3]. However, in outer space conditions the influence of ionizing radiation on the properties of IL becomes important.

Ionic liquids are composed of an organic cation $[C]^+$ and organic or inorganic anion $[A]^-$. In the present work, we use the notation [C][A] for ion pairs. Such ion pairs are also called IL

molecules by several authors. Although ILs have very low vapor pressures at room temperature, vaporization does occur at elevated temperatures and gas-phase experiments are possible [4]. There are some experimental studies of gaseous ILs made by mass spectrometry (e.g., [5-7] and references therein), but detailed studies of fragmentation under ionizing radiation are rather few. Both experimental [8-12] and theoretical [13-16] studies have shown that thermal vaporization of ILs produce mainly ion pairs in high vacuum. Ion pairs have also been directly observed by field ionization [12] and indirectly by soft-ionization mass spectrometry [9, 17], line-of-sight mass spectrometry [10, 18]and UV spectroscopy [19].

In this work, we study the photo-induced fragmentation processes by detecting fragment ions and their varying intensities as a function of VUV light wavelength of three different ILs: 1-Ethyl-2,3-dimethylimidazolium bis(trifluoromethylsulfonyl)imide [EMMIM][TFSI], 1-Ethyl-3-methylimidazolium trifluoromethanesulfonate [EMIM][OTf] and 1-Ethyl-3-methylimidazolium dicyanamide [EMIM][DCA]. The chemical structures of these ILs are shown on Figure 1.

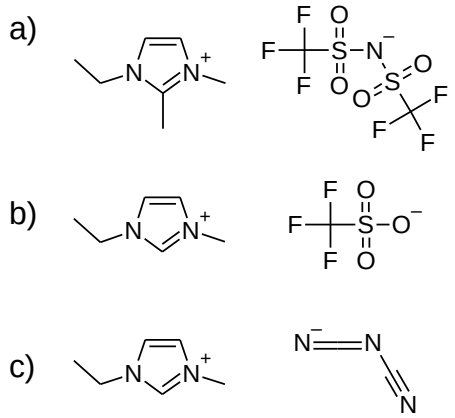


Figure 1. The chemical structures of a) [EMMIM][TFSI], b) [EMIM][OTf] and c) [EMIM][DCA].

[EMMIM][TFSI] has promising applications in fuel cells [20] and rechargeable lithium batteries [21]. [EMIM][OTf] has been studied as a electrolyte in electrochemical double-layer capacitors [22] and batteries [23]. [EMIM][DCA] can be used as a lubricant in vacuum [2], in fuel desulfurization [24], propulsion [25] and electrochemical deposition [26].

For practical applications, the stability of the ILs is important. They can have different chemical and structural weaknesses. For example, it has been suggested that the primary degradation pathway for the $[EMIM]^+$ cation in dry conditions is nucleophilic attack on the C2 position [27]. To prevent this, methylation of the $[EMIM]^+$ C2 position can be used to substitute the acidic hydrogen, which will prevent the formation of the N-heterocyclic carbene. This methylation of the $[EMIM]^+$ cation to form the $[EMMIM]^+$ cation increases the chemical stability of the IL, but also prevents hydrogen bonding interactions between the cation and anion. [28, 29]

Adding or removing functional groups can have a large impact on the physiochemical properties and chemical stability of the molecule. Noack et. al [28] have shown that the previously mentioned methylation decreases the electron density at the C2 position (the carbon atom between the two nitrogen atoms) and increases the density at the C4 and C5 positions. This electron density redistribution increases the regularity of the system, decreases the entropy and reduces the number of configurational conformers. The anion prefers to be above or below

the imidazole ring and less in the co-planar configuration with the anion near the C2 position. In the macroscopic scale, this methylation results in an increased viscosity and a higher melting point.

The aim of this study is to identify the fragmentation pathways of $[EMIM]^+$ and $[EMMIM]^+$ cations and to compare the effect of different anions on the photofragmentation channels. To the best of our knowledge, there are no previous TOF-MS (time-of-flight mass spectrometry) studies of [EMMIM][TFSI] and [EMIM][OTf], but the TOF-MS spectra of [EMIM][DCA] have been previously reported by Chambreau et al in [30], where photons in the energy range 7.4 to 10.0 eV were used as the excitation source. The electronic structure and fragmentation of the similar IL, [EMIM][TFSI], has been studied extensively [8, 31-34].

Using comparable methods we have previously investigated the fragmentation of different molecules [35, 36] and ILs such as [EMIM][BF4] [37]. In our recently published article, the vapor phase structures of several ILs, including [EMMIM][TFSI], [EMIM][OTf] and [EMIM][DCA] have been predicted using hybrid-DFT (see figure 2) and good agreement was found between the experimental UPS (Ultraviolet Photoemission Spectroscopy) and the calculated electronic structures [38, 39].
`

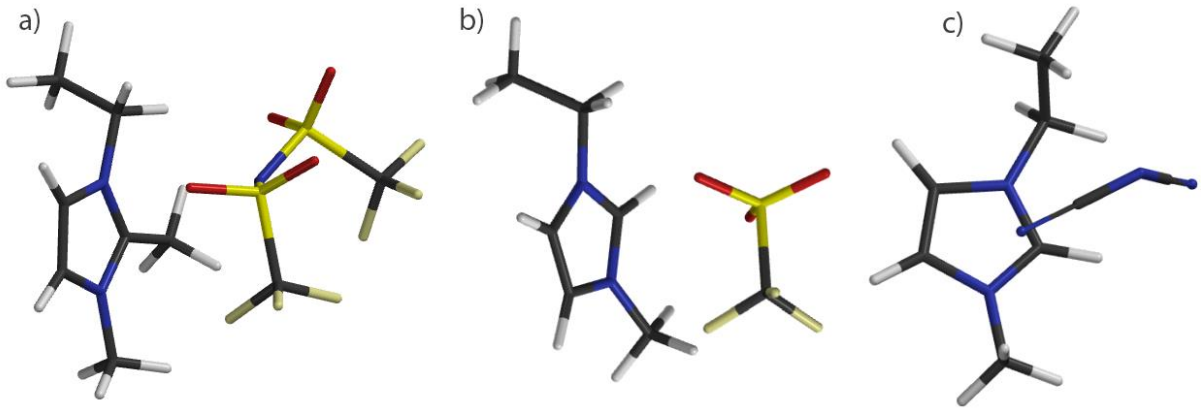


Figure 2. Predicted ion pair structures using hybrid-DFT of a) [EMMIM][TFSI], b) [EMIM][OTf] and c) [EMIM][DCA]. Carbon, nitrogen, hydrogen, sulfur and oxygen atoms are represented by black, blue, white, yellow and red colors. Reproduced with permission from Kuusik et al ACS Omega, 2021. **6**(8): p. 5255. [38]

## 2. Experimental

[EMMIM][TFSI] (purity 99.90%), [EMIM][OTf] (purity 99%) and [EMIM][DCA] (purity 98%) were purchased from IoLiTec Ionic Liquids Technologies GmbH, Germany. The chemical structures of the ILs under study are shown in Figure 1.

ILs are generally hygroscopic. Therefore, the sealed IL bottles were opened immediately before introducing the IL into the effusion cell, and the cell was mounted in the vacuum system, which was pumped down as quickly as possible. About 1.5 ml of IL sample was injected into 10 ml quartz crucibles in a fume hood. The ILs were exposed to ambient air for 5-10 minutes during the sample transportation. Gas-phase IL ion pairs were generated using thermal vaporization

with an effusion cell (model NETZ-40 from MBE Components). A liquid nitrogen cold trap was used during the measurements to lower the base pressure in the experimental chamber.

The ILs were vacuum dried inside the analysis chamber at 110 °C overnight to reduce the water content. The temperature for the experiment of each IL was chosen for optimal detector signal intensity and optimal analyzer chamber pressure in the $10^{-7}$ mbar range. During the experiment the following parameters were used:

[EMMIM][TFSI] was dried in vacuum for 11 hours at 180 °C prior to measurements. The pressure in the experimental chamber was around $4*10^{-7}$ mbar during the measurements. Maximum temperature of the effusion cell was 220 °C during the TOF-MS measurements. The color of the IL had changed from clear transparent to dark brown (with sediment) during the experiment (duration 9 h). This indicates that some thermal degradation processes occurred during the above-mentioned conditions.

[EMIM][OTf] was dried in vacuum for 12 hours at 110 °C prior to measurements. The pressure in the experimental chamber was around $8*10^{-7}$ mbar during the measurements. Maximum temperature of the effusion cell was 245 °C during the TOF-MS measurements. The color of the IL had changed from clear transparent to clear orange color during the experiment (duration 10 h).

[EMIM][DCA] was dried in vacuum for 12 hours at 110 °C prior to measurements. The pressure in the experimental chamber was around $2*10^{-7}$ mbar during the measurements. Maximum temperature of the effusion cell was 140 °C during the TOF-MS measurements. The color of the IL had changed from clear transparent to opaque black and a dark red film had formed on the crucible's walls during the experiment (duration 11 h).

Thermogravimetric analysis has shown that the thermal decomposition onset for the ILs are, 266.0–284.0 °C for [EMIM][OTf] [40] and 284 °C for [EMIM][DCA] in nitrogen environment [41]. The thermal stability of the above mentioned ILs has been investigated [42-45]. No thermogravimetric analysis for [EMMIM][TFSI] has been published, but [PMMIM][TFSI] with onset temperature of 462 °C [42] should be a close approximation. $[PMMIM]^+$ (1,2-Dimethyl-3-propylimidazolium) has one more carbon atom in the alkyl chain compared to $[EMMIM]^+$ which should not affect the thermal properties of the IL considerably [46].

The maximum operation temperature for 24 hours was experimentally determined by isothermal thermogravimetric analysis to be between 120 and 160 °C for [EMIM][DCA] [41]. We monitored changes in the TOF-MS spectra over time to understand the effects of thermal decomposition on the measurements. For [EMMIM][TFSI] and [EMIM][OTf] no major changes in the spectra were observed. However, for [EMIM][DCA] changes in the relative intensities of the peaks over time were detected, possibly due to thermal decomposition of the IL.

The TOF-MS measurements were carried out at the FinEstBeAMS beamline of the MAX-IV 1.5 GeV storage ring [47]. The beamline is equipped with a collimating grazing incidence plane grating monochromator and toroidal focusing mirrors. A 92 l/mm grating was used which covers the energy range from 4.5 eV to 50 eV. In the experiments, the following filters were used in the given photon energy ranges to suppress any higher order radiation coming from the monochromator: $MgF_2$ in 5.5-10.7 eV, In in 11.2-16.5 eV, and Sn in 18-24 eV.

The ion TOF spectra were recorded using a Wiley-McLaren TOF mass spectrometer equipped with a RoentDek GmbH 75mm active area MCP (microchannel plate) and Hexanode delay line detector. The flight times of the positive ions were used to determine their masses. Data acquisition is based on high-bandwidth waveform signal capture from the ion detector directly to the acquisition computer. In the present experiments, the time resolution was 1 ps. Our TOF-MS set-up can only detect positive ions and will not detect any neutral fragments or negatively charged ions.

The main benefits of using synchrotron VUV light as an excitation source for TOF-MS are high intensity and tunability of the excitation photon energy. The high sensitivity of VUV TOF-MS enables the detection of thermal decomposition products well below the thermal decomposition onset temperature determined via differential scanning calorimetry (DSC) and TGA [48].

## 3. Results and Discussion

### 3.1. Photoionization

Isolated ion pairs can be prepared in the gas phase by thermal vaporization [49]. Previous studies [8, 10-13, 15, 50] have shown that IL vapors are composed of neutral ion pairs under moderately high temperature and low pressure.

We claim that the IL vapors in this experiment contain neutral ion pairs, [C][A]. Here the notation [C][A] denotes a bound ion pair of a positively charged cation, $[C]^+$, and a negatively charged anion, $[A]^-$. Indirect evidence for the vaporization of isolated neutral ion pairs is provided by the UPS experiments [38] performed in the same conditions. In addition, we observed no detectable signal with the TOF analyzer without VUV light.

When the sample is irradiated by VUV photons, there are two main mechanisms that can produce intact cations $[C]^+$. The first process is the photoexcitation of the IL followed by the possible dissociation to an intact cation and anion:

$$[C][A] + h\nu \rightarrow [C][A]^* \rightarrow [C]^+ + [A]^- \qquad (1)$$

The second mechanism is the photoionization of the ion pair, which generates intact cations by dissociation:

$$[C][A] + h\nu \rightarrow [C]^+ + [A]^\bullet + e^- \qquad (2)$$

Since both of these mechanisms also generate various other ions resulting from fragmentation, TOF-MS is an excellent experimental method to study these processes.

### 3.1 [EMMIM][TFSI]

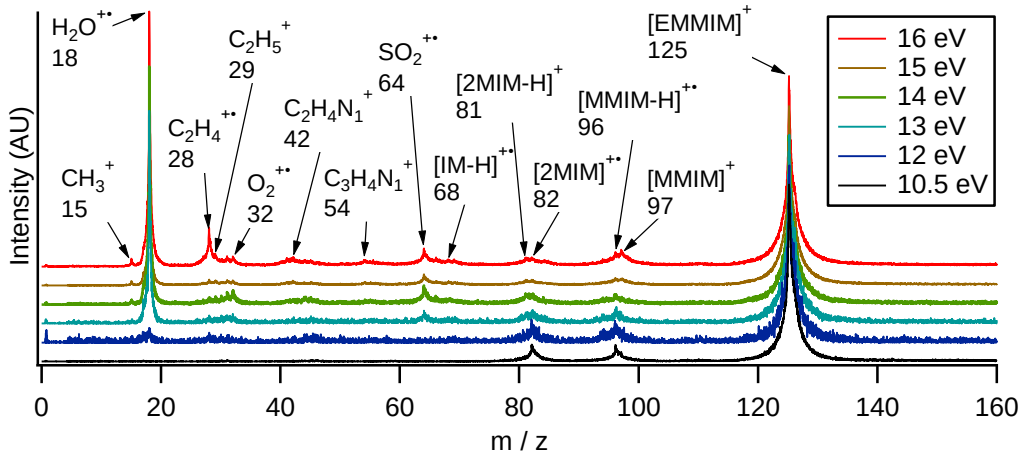


Figure 3. TOF-MS spectra of [EMMIM][TFSI]. The spectra have been normalized to m/z 125 peak height and offset vertically. Excitation photon energies and key fragments are given in the figure.

TOF-MS spectra of [EMMIM][TFSI] (see figure 3) were acquired with 10.5, 12, 13, 14, 15, 16 eV photon energies at the temperature of 200 °C. Due to the relatively low photon energies and intensities used for the photoexcitation, only singly charged ions are present in the spectra.

The intact $[EMMIM]^+$ cation peak was identified at m/z 125 and the cation fragments were observed at m/z 42, 54, 68, 81, 82, 96, 97. The peak at m/z 81 is assigned to $[2MIM\text{-}H]^+$ (dehydrogenated 2-Methylimidazolium, $C_4H_5N_2^+$). The peak at m/z 82 is assigned to $[2MIM]^{+\bullet}$ (2-Methylimidazolium, $C_4H_6N_2^{+\bullet}$). The peak at m/z 96 is assigned to $[MMIM\text{-}H]^{+\bullet}$ (dehydrogenated 2,3-Dimethylimidazolium, $C_5H_8N_2^{+\bullet}$). The peak at m/z 97 is assigned to $[MMIM]^+$ (2,3-Dimethylimidazolium, $C_5H_9N_2^+$). The peak at m/z 68 is assigned to $[IM\text{-}H]^{+\bullet}$ (dehydrogenated imidazolium, $C_3H_4N_2^{+\bullet}$). During the fragmentation of EMMIM and EMIM based ILs the aromatic imidazolium ring can remain intact or it may break. For example, the imidazolium ring is intact in the latter fragments, but the fragments at m/z 42 ($C_2H_4N^+$) [51] and 54 ($C_3H_4N^+$) result from the breaking of the imidazolium ring [52]. The observed fragmentation pathways are graphically represented on figure S1.

One would expect to observe a fragment at m/z 111, because the typical fragmentation pattern for a similar IL, [EMIM][TFSI], involves the loss of the methyl group from the nitrogen position [53]. However, no $[EMIM]^+$ peak at m/z 111 was detected. We propose that fragmentation pathways that involve the loss of the ethyl group are so much more probable that the m/z 111 fragment was undetectable in this experiment.

We suggest that the peak at m/z 82 should be assigned to 2-Methylimidazolium and not 3-Methylimidazolium, because TOF-SIMS experiments have demonstrated that imidazolium based ILs have the highest probability to fragment from the longest alkyl chain in N positions and C-C bonds have an order of magnitude lower probability to break [52]. Our suggestion is supported by the values of average bond energies: 3.6 eV (347 kJ/mol) for the C-C bond and 3.2 eV (305 kJ/mol) for the N-C bond [54].

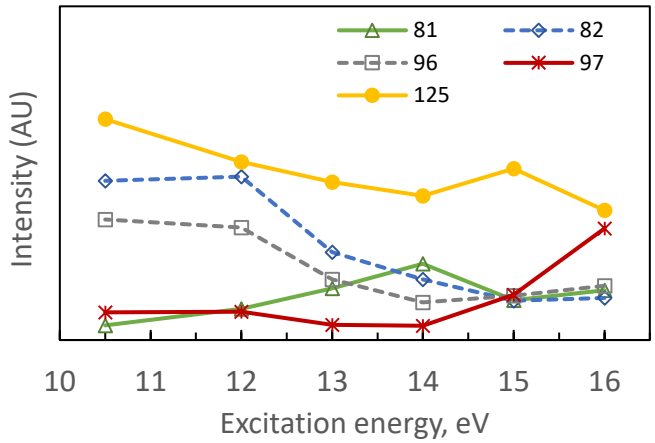


Figure 4. The relative intensity (peak intensity relative to the sum of IL related fragments) of the main fragments of [EMMIM][TFSI] as a function of excitation energy. Dotted lines represent odd-electron fragments and solid lines even-electron fragments. The m/z 125 curve has been multiplied by 0.1 for better visual comparison.

Several noteworthy behaviors can be deduced from the data in Figure 4. It is evident, that the intensities of the $[2MIM]^{+\bullet}$ peak at m/z 82 and the dehydrogenated $[MMIM\text{-}H]^{+\bullet}$ peak at m/z 96 have very similar excitation energy dependencies. Both of these fragments are odd-electron cations. Therefore, they are fragmentation pathways from the same initial state. This means that after ionization or excitation the ion-pair can fragment by losing either the ethyl group or both the ethyl group and methyl group from the nitrogen positions. These are competing decay channels with approximately equal probability. The main $[EMMIM]^+$ cation peak at m/z 125 and the $[MMIM]^+$ peak at m/z 97 behave somewhat similarly, but differ around 15 eV. Therefore, it is difficult to make clear conclusions about those fragments. The dehydrogenated $[MIM\text{-}H]^{+\bullet}$ peak at m/z 81 behaves differently from all the other fragmentation channels. No hydrogenated fragments were detected for [EMMIM][TFSI].

The origin of dehydrogenated $[2MIM\text{-}H]^{+\bullet}$ fragments is not clear. The first possibility is that dehydrogenation occurs during the heating and evaporation process in the crucible similarly as with $[EMIM][BF_4]$ [41]. The second possibility is that dehydrogenated species are the result of different fragmentation pathways. The detailed mechanism is not fully understood [41].

### 3.2 [EMIM][OTf]

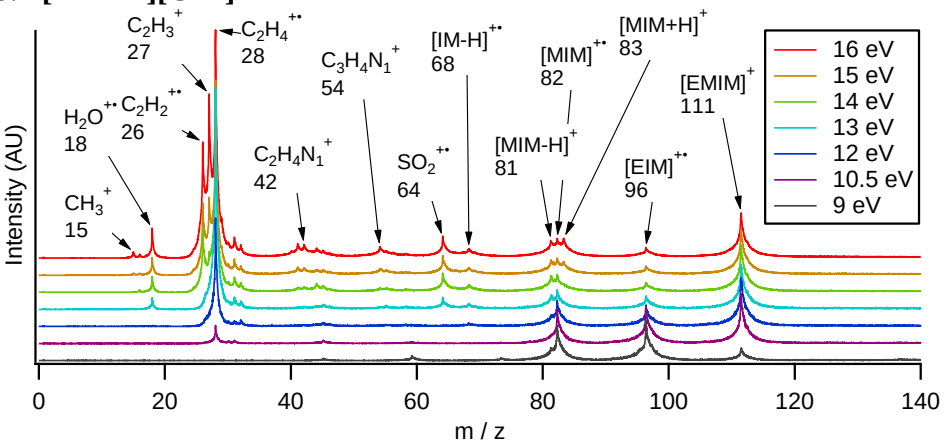

Figure 5. TOF-MS spectra of [EMIM][OTf]. The spectra have been normalized to the m/z 111 peak height and offset vertically, except the 9 eV curve which has not been normalized. Excitation photon energies and key fragments are given in the figure.

A weak signal of $[EMIM\text{-}H]^{+\bullet}$ at 110 = m/z was detected already at 110 °C during heating, which originates from the modification of the IL by the residuals inside the IL [30]. The TOF-MS were measured using 9, 10.5, 12, 14, 15 and 16 eV photon energies at the temperature 243 °C, where the residual products were not observed and the main signal originates from the vaporized [EMIM][OTf] ion pairs (Figure 5).

The peaks at m/z 68, 81, 82, 83, 96 and 111 correspond to $[IM\text{-}H]^{+\bullet}$ (dehydrogenated imidazolium), $[MIM\text{-}H]^{+}$, $[MIM]^{+\bullet}$, $[MIM+H]^{+}$, $[EIM]^{+\bullet}$ (1-Ethylimidazolium) and $[EMIM]^{+}$, respectively (see Supplementary Figure S1). Besides the separation of the anion and cation from the ion pair, three fragmentation channels can be identified. The first one involves the loss of the methyl ($-CH_3$) group and produces $[EIM]^{+\bullet}$ fragments. The second one involves the loss of the ethyl ($-C_2H_5$) group and produces $[MIM\text{-}H]^{+}$, $[MIM]^{+\bullet}$ or $[MIM+H]^{+}$ fragments. At excitation energies 15 and 16 eV the corresponding triple peak feature at m/z 81-83 can be clearly observed (Figure 5). The third fragmentation channel involves the loss of both alkyl groups and produces $[IM\text{-}H]^{+\bullet}$.

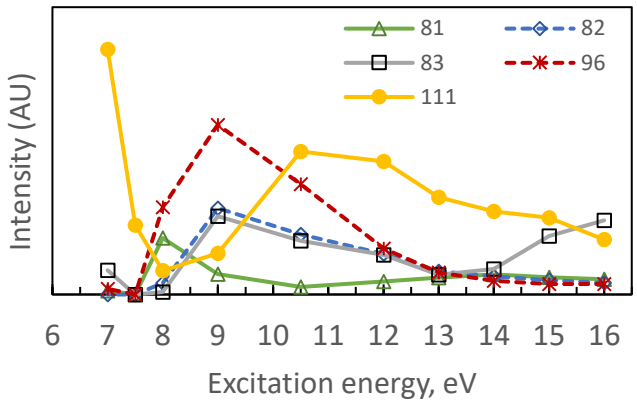


Figure 6. The relative intensity (peak intensity relative to the sum on IL related fragments) of the main fragments of [EMIM][OTf] as a function of excitation energy. Dotted lines represent odd electron fragments and solid lines even electron fragments. The m/z 83 curve has been multiplied by 4 for better visual comparison.

The energy dependence of the main fragments of [EMIM][OTf] (Figure 6) will be discussed next. Firstly, the way how the main intact cation peak intensity varies over energy is interesting. At low energies, its intensity is high, then it drops significantly at around 9 eV and then rises again. We interpret this analogously to our previous study of $[EMIM][BF_4]$ in [37]. When the photon energy is below the ionization threshold, but over the first photoexcitation resonance, the ion-pairs are photoexcited and they can fragment to their cation and anion constituents (according to eq. 1). When the photon energy is raised over the photoexcitation threshold energy but it is still below the ionization energy, the signal decreases as the photoabsorption cross section decreases. Starting from the photoionization threshold the cation peak signal starts to increase again. This analysis is based on the assumption that there are many excited states below the ionization threshold, similarly to [EMIM][BF4][37]. These states are dissociative and result in various fragments. An extensive study of excited states of several ILs using EELS, UPS and DFT [55] further supports this analysis. Unfortunately, the lack of sufficient data points prevents us from determining the ionization energy exactly but it is approximately 10 eV.

Secondly, the two dominant cation fragmentation peaks at m/z 96 and m/z 82 seem to behave similarly. Therefore, we assume that the fragmentation to $[MIM]^{+\bullet}$ and $[EIM]^{+\bullet}$ are probabilistic outcomes from the same initial state.

Thirdly, the $[MIM]^{+\bullet}$ at m/z 82 and the hydrogenated $[MIM+H]^{+}$ peak at m/z 83 behave almost identically at low energies. From about 14 eV onwards the $[MIM+H]^{+}$ diverges to higher intensity compared to its m/z 82 counterpart. Therefore, the fragmentation to $[MIM]^{+\bullet}$ or to $[MIM+H]^{+}$ seem to be competing decay channels and when there is more energy deposited, the system seems to prefer the $[MIM+H]^{+}$ fragmentation channel.
We draw the following conclusion from these behaviors: there is no reason to assume the presence of a hydrogenated [EMIM][OTf] in the liquid phase, as the $[MIM]^{+\bullet}$ and $[MIM+H]^{+}$ peaks are naturally explained.

However, the presence of dehydrogenated [EMIM][OTf] cannot be ruled out. A weak signal of the $[EMIM-H]^{+\bullet}$ at 110 = m/z was detected already at 110 °C during heating. This peak can originate from the modification of the ionic liquid by the residuals inside the IL [30].The dehydrogenated $[MIM-H]^{+}$ peak at m/z 81 behaves differently from other peaks (Figure 6). Its intensity seems to be anti-correlated to the intensity of the $[EMIM]^{+}$ peak at m/z 111 and therefore it could result from thermal decomposition products. Furthermore, unlike in the case of [EMIM][$BF_4$] [37], the dehydrogenated $[EIM-H]^{+\bullet}$ at m/z 95 is not observed in [EMIM][OTf].

### 3.3 [EMIM][DCA]

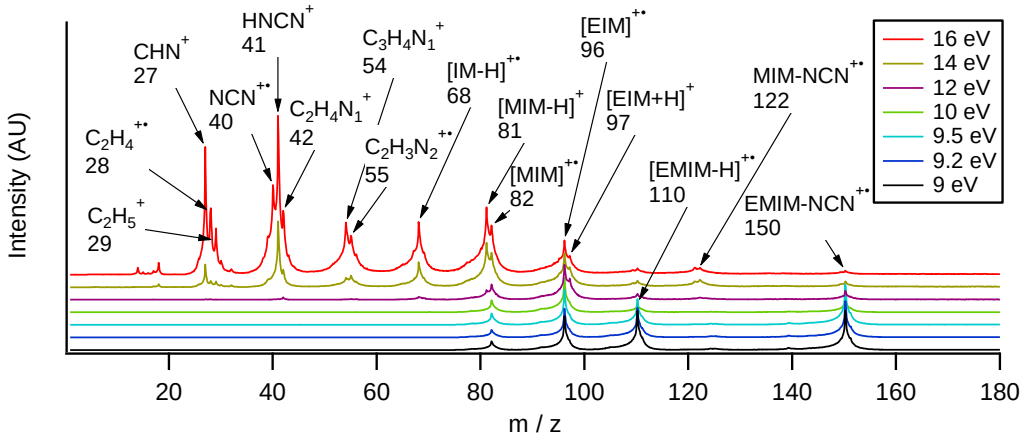


Figure 7. TOF-MS spectra of [EMIM][DCA]. The spectra have been normalized to m/z 96 peak height and offset vertically. Excitation photon energies and key fragments are given in the figure.

The TOF-MS spectra of [EMIM][DCA] were acquired with 9, 9.2, 9.5, 10.5, 12, 14 and 16 eV excitation energies (Figure 7). The same m/z 82, 96, 110, 122, 150 peaks as in the Chambreau *et al.* experiment [30] were observed in our [EMIM][DCA] TOF-MS spectra. Peaks at m/z 68, 81, 82, 96, 97, 110, 111, 121, 122 and 150 correspond to $[IM-H]^{+\bullet}$, $[MIM-H]^{+}$, $[MIM]^{+\bullet}$, $[EIM]^{+\bullet}$, $[EIM+H]^{+}$, $[EMIM-H]^{+\bullet}$, $[EMIM]^{+}$, MIM-NCN-$H^{+}$ (dehydrogenated 2-cyanoimino-3-methylimidazole), MIM-$NCN^{+\bullet}$ (2-cyanoimino-3-methylimidazole) and EMIM-$NCN^{+}$ (2-cyanoimino-1-Ethyl-3-methylimidazole, NCN-ylidene).

The $[EIM]^{+\bullet}$ fragment at m/z 96 and the hydrogenated $[EIM+H]^{+}$ fragment at m/z 97 have very similar energy dependencies (see supplementary figure S3). We draw a similar conclusion as in the [EMIM][OTF] case from this data: the fragmentation to $[EIM]^{+}$ or to $[EIM+H]^{+}$ seem to be competing decay channels from the same initial state. Again, there is no need to suppose the presence of hydrogenated [EMIM][DCA] but rather the the $[EIM+H]^{+}$ peak results from the cleavage of the methyl group when it leaves a hydrogen behind (i.e a net loss of $CH_2$).

It is likely that the peak at m/z 150 is a liquid phase reaction product [30, 56], $EMIM\text{-}NCN^{+\bullet}$ (NCN-ylidene), involving the carbene intermediate. It is well-known that carbenes are highly reactive [57, 58]. The mechanism proposed by Chambreau *et al.* involves the proton transfer from $[EMIM]^{+}$ to the $[DCA]^{-}$ anion to form HDCA. This is followed by the rapid nucleophilic attack by EMIM**:** to the carbon in HDCA. The inner nitrogen of HDCA can migrate to C2 on the imidazole ring, followed by the elimination of HCN, resulting in the formation of $EMIM\text{-}NCN^{+\bullet}$ [30]. $EMIM\text{-}NCN^{+\bullet}$ is a proposed thermal decomposition product of [EMIM][DCA] because there is strong evidence that the $[DCA]^{-}$ anion can cause $S_N2$ dealkylation of imidazolium [30, 59, 60]. In addition, dynamics simulations and statistical modeling of thermal decomposition of [EMIM][DCA] provide a theoretical explanation for the formation of EMIM**:** (dehydrogenated EMIM carbene) via transfer of the C2 proton of $[EMIM]^{+}$ to $[DCA]^{-}$ [56].

Therefore, we also suggest that the reaction product EMIM-NCN is formed in liquid phase and is not a result of gas phase interactions. The experimental chamber pressure was increasing over time even when the effusion cell temperature was kept constant for 4 hours during the experiment. In our experience if the only process involved is thermal evaporation then the experimental chamber pressure should decrease over time as the water evaporates from the IL and there is outgassing from the vacuum chamber's inner surface. The constant increase in the pressure over time can be caused by thermal decomposition of the IL or chemical reactions inside the IL. As the experiment was carried out at 140 °C, well below the 284 °C thermal decomposition temperature of [EMIM][DCA] [41], a plausible explanation is that the decrease of the water content creates an environment where chemical reactions can take place to produce $EMIM\text{-}NCN^{+\bullet}$. This could be a useful one-pot synthesis method for NCN imidazolium-ylidene species without the need for flammable solvents at lower temperature than reported previously [30]. We observed the $EMIM\text{-}NCN^{+\bullet}$ reaction product already at 140 °C in contrast to the TOF-MS experiment of Chambreau *et al.*, which was conducted at 200 °C effusive source temperature. We suspect that this could be due to the longer vacuum drying process by us. The vacuum drying process of [EMIM][DCA] was not mentioned in the publication [30].
The peaks at m/z 121 and 122 are the fragments resulting from loss of an ethyl group from the $EMIM\text{-}NCN^{+\bullet}$ reaction product. This assignment is based on the fact that the fragment has a m/z 28 difference from the $EMIM\text{-}NCN^{+\bullet}$ parent compound, which indicates a loss of an ethyl group. As with $[EMIM]^{+}$ fragments involving alkyl group losses, the dehydrogenated species $MIM\text{-}NCN\text{-}H^{+\bullet\bullet}$ can be also observed at m/z 121. The peak at m/z 110 is assigned to $[EMIM\text{-}H]^{+\bullet}$. The structures of the fragments are represented in supplementary Figure S3.

### 3.4 Comparison of ILs

Deyko *et al*. concluded that the intact cation to main fragment ratio seems to depend on the size of the anion [6]. It is of interest to compare the intensity of the intact cation peak to the sum of the areas of the main cation fragments ($[MIM]^{+\bullet}$, $[MMIM]^{+}$, $[EIM]^{+\bullet}$). The ratio was highest for [EMMIM][TFSI] and lowest for [EMIM][DCA]. Tolstogouzov *et al*. performed a TOF-MS experiment on [EMIM][TFSI] using 20 eV electron ionization and observed a fragment to parent cation ratio similar to our results of [EMMIM][TFSI] [61]. However, a 70 eV

electrospray ionization line-of-sight 1MS experiment of [EMIM][TFSI] demonstrated a lower ratio [6]. Our experiment seems to confirm this hypothesis: ILs with larger anions have less cation fragmentation.

TOF-SIMS spectra of [EMIM][TFSI] have been reported [31, 32, 62]. Both 2 keV $He^+$ and 2.5 keV $Ga^+$ was used for excitation. The cation fragment peak assignment looks remarkably similar to our [EMIM][OTf] TOF-MS spectra with 16 eV excitation energy. The cation fragments have less intensity in the TOF-SIMS study of [EMIM][TFSI] when compared to our [EMIM][OTf], but the main fragment peaks $[MIM]^{+\bullet}$, $[MIM+H]^+$ and $[EIM]^{+\bullet}$ peaks seem to be in roughly the same proportion in respect to each other [32]. The main difference with our results is the higher intensity of peaks at m/z 40-42 and 52-56. The peaks in these regions are associated with the fragmentation of the imidazolium ring. Breakup of the ring is more probable with higher energy ions.

The additional peaks from $EMIM\text{-}NCN^{+\bullet}$ in the TOF-MS spectra of [EMIM][DCA] makes it difficult to compare [EMIM][DCA] and [EMIM][OTf] directly. Both $[EMIM]^+$ based ILs produce preferably $[EIM]^{+\bullet}$ fragments at lower (below 12 eV) excitation energies. In addition, [EMIM][OTf] exhibits a triple peak feature for $[MIM\text{-}H]^+$, $[MIM]^{+\bullet}$ and $[MIM+H]^+$. The $[EMIM]^+$ cation and the hydrogenated $[MIM+H]^+$ are not present in [EMIM][DCA], but the hydrogenated $[EIM+H]^+$ and dehydrogenated $[EMIM\text{-}H]^+$ fragments are observed. [EMMIM][TFSI] produces different fragments than $[EMIM]^+$ based ILs: $[MMIM\text{-}H]^+$ and $[MMIM]^+$ are observed and no hydrogenated species are detected.

## 5. Conclusions

A TOF-MS study on the fragmentation of [EMMIM][TFSI], [EMIM][OTf] and [EMIM][DCA] ionic liquids has been successfully carried out using photoexcitation with energies from 9 to 16 eV. VUV induced fragmentation of vapor phase imidazolium-based ionic liquids gives rise to various ions corresponding to different fragmentation pathways. The largest intensity of the intact cation peak relative to the sum of the areas of the other cation fragments was detected in the case of [EMMIM][TFSI]. Our experiment seems to confirm the hypothesis that the ILs with larger anions have less cation fragmentation.

In case of [EMMIM][TFSI] the loss of a methyl group from the nitrogen position should produce a $[EMIM]^+$ peak at m/z 111. However, unexpectedly in [EMMIM][TFSI] we did not observe this peak in the photon energy range of 10.5 to 16 eV.

Even at low temperatures of 140 °C, the temperature induced reaction product 2-cyanoimino-1-Ethyl-3-methylimidazole at m/z 150 was observed in the TOF-MS spectra of [EMIM][DCA].

[EMIM][OTf] exhibits a triple peak feature consisting of $[MIM\text{-}H]^+$, $[MIM]^+$ and $[MIM+H]^+$. The $[MIM]^+$ and $[MIM+H]^+$ fragments of [EMIM][OTf] were seen to behave very similarly with respect to excitation energy. This is also the case for $[EIM]^+$ and $[EIM+H]^+$ fragments in [EMIM][DCA]. We conclude that in each case they result from the same initial state and there is no need to assume the presence hydrogenated [EMIM][DCA] or [EMIM][OTf] species in the liquid phase.

[EMMIM][TFSI] produces different fragments than $[EMIM]^+$ based ILs: $[MMIM\text{-}H]^+$ and $[MMIM]^+$ are observed and no hydrogenated species are detected.

**Acknowledgements**

The authors gratefully acknowledge the financial support by the Estonian Research Council (IUT2-25, MOBTP145), Estonian Centre of Excellence in Research "Advanced materials and high-technology devices for sustainable energetics, sensorics and nanoelectronics" TK141 (2014-2020.4.01.15-0011), European Regional Development Fund (project " Developing new research services and research infrastructures at MAX IV synchrotron radiation source" (2014-2020.4.01.20-0278) and the University of Tartu ASTRA Project PER ASPERA financed by the European Regional Development Fund. The research leading to this result has been also supported by the project CALIPSOplus under the Grant Agreement 730872 from the EU Framework Programme for Research and Innovation HORIZON 2020. The authors wish to thank the staff of the MAX-IV laboratory for support during measurements.

## References


1. Hayes, R., G.G. Warr, and R. Atkin, *Structure and Nanostructure in Ionic Liquids.* Chemical Reviews, 2015. **115**(13): p. 6357-6426.
2. Kawada, S. and S. Sasaki, *Tribological Properties of Cyano-Based Ionic Liquids under Different Environments.* Tribology Online, 2018. **13**(3): p. 152-156.
3. Zhou, F., Y. Liang, and W. Liu, *Ionic liquid lubricants: designed chemistry for engineering applications.* Chemical Society Reviews, 2009. **38**(9): p. 2590-2599.
4. Earle, M., et al., *The distillation and volatility of ionic liquids.* Nature, 2006. **439**(7078): p. 831-834.
5. Cooper, R., et al., *IR and UV Spectroscopy of Vapor-Phase Jet-Cooled Ionic Liquid emim (+) Tf2N (-): Ion Pair Structure and Photodissociation Dynamics.* Journal of Physical Chemistry A, 2013. **117**(47): p. 12419-12428.
6. Deyko, A., et al., *The vapour of imidazolium-based ionic liquids: a mass spectrometry study.* Physical Chemistry Chemical Physics, 2011. **13**(37): p. 16841-16850.
7. Neto, B.A.D., et al., *Vapors from Ionic Liquids: Reconciling Simulations with Mass Spectrometric Data.* Journal of Physical Chemistry Letters, 2012. **3**(23): p. 3435-3441.
8. Strasser, D., et al., *Photoelectron spectrum of isolated ion-pairs in ionic liquid vapor.* J Phys Chem A, 2007. **111**(17): p. 3191-5.
9. Chambreau, S.D., et al., *Heats of vaporization of room temperature ionic liquids by tunable vacuum ultraviolet photoionization.* J Phys Chem B, 2010. **114**(3): p. 1361-7.
10. Armstrong, J.P., et al., *Vapourisation of ionic liquids.* Phys Chem Chem Phys, 2007. **9**(8): p. 982-90.
11. Leal, J.P., et al., *The nature of ionic liquids in the gas phase.* J Phys Chem A, 2007. **111**(28): p. 6176-82.
12. Gross, J.H., *Molecular ions of ionic liquids in the gas phase.* J Am Soc Mass Spectrom, 2008. **19**(9): p. 1347-52.
13. Kelkar, M.S. and E.J. Maginn, *Calculating the enthalpy of vaporization for ionic liquid clusters.* J Phys Chem B, 2007. **111**(32): p. 9424-7.
14. Koddermann, T., D. Paschek, and R. Ludwig, *Ionic liquids: dissecting the enthalpies of vaporization.* Chemphyschem, 2008. **9**(4): p. 549-55.
15. Ballone, P., et al., *Neutral and charged 1-butyl-3-methylimidazolium triflate clusters: equilibrium concentration in the vapor phase and thermal properties of nanometric droplets.* J Phys Chem B, 2007. **111**(18): p. 4938-50.
16. Koddermann, T., D. Paschek, and R. Ludwig, *Molecular dynamic simulations of ionic liquids: a reliable description of structure, thermodynamics and dynamics.* Chemphyschem, 2007. **8**(17): p. 2464-70.
17. Strasser, D., et al., *Tunable Wavelength Soft Photoionization of Ionic Liquid Vapors.* Journal of Physical Chemistry A, 2010. **114**(2): p. 879-883.
18. Lovelock, K.R., et al., *Vaporisation of a dicationic ionic liquid.* Chemphyschem, 2009. **10**(2): p. 337-40.
19. Wang, C., et al., *Direct UV-spectroscopic measurement of selected ionic-liquid vapors.* Phys Chem Chem Phys, 2010. **12**(26): p. 7246-50.
20. Sandoval, A.P., M.F. Suárez-Herrera, and J.M. Feliu, *Hydrogen redox reactions in 1-ethyl-2,3-dimethylimidazolium bis(trifluoromethylsulfonyl)imide on platinum single crystal electrodes.* Electrochemistry Communications, 2014. **46**: p. 84-86.
21. Sandoval-Rojas, A.P., M.F. Suárez-Herrera, and J.M. Feliu, *Catalysis of poly(3,4-ethylenedioxythiophene)-Pt(hkl) electrodes towards 2,5-dimercapto-1,3,4-thiadiazole in 1-ethyl-2,3-dimethylimidazolium bis(trifluoromethylsulfonyl)imide.* Electrochimica Acta, 2016. **218**: p. 54-57.

22. Mousavi, M.P.S., et al., *Ionic Liquids as Electrolytes for Electrochemical Double-Layer Capacitors: Structures that Optimize Specific Energy.* Acs Applied Materials & Interfaces, 2016. **8**(5): p. 3396-3406.
23. Huang, Y., et al., *Developing Dual‐Graphite Batteries with Pure 1‐Ethyl‐3‐methylimidazolium Trifluoromethanesulfonate Ionic Liquid as the Electrolyte.* ChemElectroChem, 2019. **6**(17): p. 4681-4688.
24. Diabate, P., et al., *Novel Task Specific Ionic Liquids to Remove Heavy Metals from Aqueous Effluents.* Metals, 2018. **8**(6): p. 412.
25. Li, J., et al., *The ignition process measurements and performance evaluations for hypergolic ionic liquid fuels: [EMIm][DCA] and [BMIm][DCA]*. Fuel, 2018. **215**: p. 612-618.
26. Leong, T.-I., et al., *Electrochemical Study of Copper in the 1-Ethyl-3-Methylimidazolium Dicyanamide Room Temperature Ionic Liquid.* Journal of The Electrochemical Society, 2008. **155**(4): p. F55.
27. Ye, Y. and Y.A. Elabd, *Relative Chemical Stability of Imidazolium-Based Alkaline Anion Exchange Polymerized Ionic Liquids.* Macromolecules, 2011. **44**(21): p. 8494-8503.
28. Noack, K., et al., *The role of the C2 position in interionic interactions of imidazolium based ionic liquids: a vibrational and NMR spectroscopic study.* Physical Chemistry Chemical Physics, 2010. **12**(42): p. 14153.
29. Fumino, K., A. Wulf, and R. Ludwig, *Strong, Localized, and Directional Hydrogen Bonds Fluidize Ionic Liquids.* Angewandte Chemie International Edition, 2008. **47**(45): p. 8731-8734.
30. Chambreau, S.D., et al., *Thermal decomposition mechanisms of alkylimidazolium ionic liquids with cyano-functionalized anions.* J Phys Chem A, 2014. **118**(47): p. 11119-32.
31. Günster, J., et al., *A time-of-flight secondary ion mass spectroscopy study of 1-ethyl-3-methylimidazolium bis(trifluoromethylsulfonyl)imide RT-ionic liquid.* Surface Science, 2008. **602**(21): p. 3403-3407.
32. Souda, R., *Phase Transition of 1-Ethyl-3-Methylimidazolium Bis(trifluoromethylsulfonyl)imide Thin Films on Highly Oriented Pyrolytic Graphite.* The Journal of Physical Chemistry B, 2009. **113**(39): p. 12973-12977.
33. Fletcher, K.A. and S. Pandey, *Surfactant Aggregation within Room-Temperature Ionic Liquid 1-Ethyl-3-methylimidazolium Bis(trifluoromethylsulfonyl)imide.* Langmuir, 2004. **20**(1): p. 33-36.
34. Höfft, O., et al., *Electronic Structure of the Surface of the Ionic Liquid [EMIM][Tf2N] Studied by Metastable Impact Electron Spectroscopy (MIES), UPS, and XPS.* Langmuir, 2006. **22**(17): p. 7120-7123.
35. Kisand, V., et al., *Fragmentation and electronic decay of vacuum-ultraviolet-excited resonant states of molecular CsCl.* Journal of Physics B-Atomic Molecular and Optical Physics, 2003. **36**(19): p. 3909-3921.
36. Osmekhin, S., et al., *Fragmentation of molecular tributyltin chloride.* International Journal of Mass Spectrometry, 2008. **273**(1-2): p. 48-52.
37. Kuusik, I., et al., *Near threshold photodissociation study of EMIMBF4 vapor.* Rsc Advances, 2015. **5**(9): p. 6834-6842.
38. Kuusik, I., et al., *Ionic Liquid Vapors in Vacuum: Possibility to Derive Anodic Stabilities from DFT and UPS.* ACS Omega, 2021. **6**(8): p. 5255-5265.
39. Kahk, J.M., et al., *Frontier orbitals and quasiparticle energy levels in ionic liquids.* npj Computational Materials, 2020. **6**(1).

40. Chong, M.Y., et al., *Enhancing the performance of green solid-state electric double-layer capacitor incorporated with fumed silica nanoparticles.* Journal of Physics and Chemistry of Solids, 2018. **117**: p. 194-203.
41. Navarro, P., et al., *Thermal Properties of Cyano-Based Ionic Liquids.* Journal of Chemical & Engineering Data, 2013. **58**(8): p. 2187-2193.
42. Fredlake, C.P., et al., *Thermophysical Properties of Imidazolium-Based Ionic Liquids.* Journal of Chemical & Engineering Data, 2004. **49**(4): p. 954-964.
43. Seoane, R.G., et al., *Temperature Dependence and Structural Influence on the Thermophysical Properties of Eleven Commercial Ionic Liquids.* Industrial & Engineering Chemistry Research, 2012. **51**(5): p. 2492-2504.
44. Merkel, N., et al., *Influence of anion and cation on the vapor pressure of binary mixtures of water+ionic liquid and on the thermal stability of the ionic liquid.* Fluid Phase Equilibria, 2015. **394**: p. 29-37.
45. Sebastián, P., et al., *Study of the interface Pt(111)/ [Emmim][NTf2] using laser-induced temperature jump experiments.* Electrochemistry Communications, 2015. **55**: p. 39-42.
46. Tokuda, H., et al., *Physicochemical Properties and Structures of Room Temperature Ionic Liquids. 2. Variation of Alkyl Chain Length in Imidazolium Cation.* The Journal of Physical Chemistry B, 2005. **109**(13): p. 6103-6110.
47. Parna, R., et al., *FinEstBeaMS - A wide-range Finnish-Estonian Beamline for Materials Science at the 1.5 GeV storage ring at the MAX IV Laboratory.* Nuclear Instruments & Methods in Physics Research Section a-Accelerators Spectrometers Detectors and Associated Equipment, 2017. **859**: p. 83-89.
48. Chambreau, S.D., et al., *Thermal Decomposition Mechanism of 1-Ethyl-3-methylimidazolium Bromide Ionic Liquid.* The Journal of Physical Chemistry A, 2012. **116**(24): p. 5867-5876.
49. Koh, C.J. and S.R. Leone, *Simultaneous ion-pair photodissociation and dissociative ionization of an ionic liquid: velocity map imaging of vacuum-ultraviolet-excited 1-ethyl-3-methylimidazolium bis(trifluoromethylsulfonyl)imide.* Molecular Physics, 2012. **110**(15-16): p. 1705-1712.
50. Strasser, D., et al., *Tunable wavelength soft photoionization of ionic liquid vapors.* J Phys Chem A, 2010. **114**(2): p. 879-83.
51. B.D., M., *A Handbook of Spectroscopic Data Chemistry (UV, IR, PMR, CNMR and Mass Spectroscopy)*. 2009: Oxford Book Company.
52. Bundaleski, N., et al., *Ion-induced fragmentation of imidazolium ionic liquids: TOF-SIMS study.* International Journal of Mass Spectrometry, 2013. **353**: p. 19-25.
53. Dunaev, A.M., et al., *Dimer neutral ion pairs and associative ions in saturated vapor of 1-ethyl-3-methylimidazolium trifluoromethanesulfonate ionic liquid.* Calphad, 2019. **65**: p. 127-131.
54. Petrucci, R.H., et al., *General Chemistry: Principles and Modern Applications*. 2016: Pearson Canada Incorporated.
55. Regeta, K., et al., *Free electrons and ionic liquids: study of excited states by means of electron-energy loss spectroscopy and the density functional theory multireference configuration interaction method.* Physical Chemistry Chemical Physics, 2015. **17**(24): p. 15771-15780.
56. Liu, J., S.D. Chambreau, and G.L. Vaghjiani, *Dynamics simulations and statistical modeling of thermal decomposition of 1-ethyl-3-methylimidazolium dicyanamide and 1-ethyl-2,3-dimethylimidazolium dicyanamide.* J Phys Chem A, 2014. **118**(47): p. 11133-44.
57. Hollóczki, O., et al., *Carbenes in ionic liquids.* New Journal of Chemistry, 2010. **34**(12): p. 3004.

58. Rodríguez, H., et al., *Reaction of elemental chalcogens with imidazolium acetates to yield imidazole-2-chalcogenones: direct evidence for ionic liquids as proto-carbenes.* Chemical Communications, 2011. **47**(11): p. 3222.
59. Emel'Yanenko, V.N., S.P. Verevkin, and A. Heintz, *The Gaseous Enthalpy of Formation of the Ionic Liquid 1-Butyl-3-methylimidazolium Dicyanamide from Combustion Calorimetry, Vapor Pressure Measurements, and Ab Initio Calculations.* Journal of the American Chemical Society, 2007. **129**(13): p. 3930-3937.
60. Deyko, A., et al., *Measuring and predicting ΔvapH298 values of ionic liquids.* Physical Chemistry Chemical Physics, 2009. **11**(38): p. 8544.
61. Tolstogouzov, A., et al., *Study on imidazolium-based ionic liquids with scanning atom probe and Knudsen effusion mass spectrometry.* Surface and Interface Analysis, 2008. **40**(13): p. 1614-1618.
62. Smith, E.F., et al., *Ionic Liquids in Vacuo: Analysis of Liquid Surfaces Using Ultra-High-Vacuum Techniques.* Langmuir, 2006. **22**(22): p. 9386-9392.